# Experimental Verification of Flywheel Power Leveling System Oriented to Low Cost and General Purpose Use


Jun-ichi Itoh
Nagaoka University of Technology
Niigata, Japan
itoh@vos.nagaokaut.ac.jp

Kenta Tanaka
Nagaoka University of Technology
Niigata, Japan
k_tanaka@stn.nagaokaut.ac.jp

Soya Matsuo
Nagaoka University of Technology
Niigata, Japan
soya_matsuo@stn.nagaokaut.ac.jp

Noboru Yamada
Nagaoka University of Technology
Niigata, Japan
noboru@nagaokaut.ac.jp



***Abstract*— This paper discusses the performances of a power leveling system with a 3.0-MJ, 9500-r/min flywheel energy storage. In term of the cost reduction, this system uses low cost flywheel and the general purpose products. Therefore, time delay that occurs in the measurement circuit can limit the control performance. In order to overcome this problem, a time delay compensation scheme based on Smith predictor is applied in order to improve the control performance. In addition, vibration characteristics during power leveling operation are evaluated in the experiment. From the results, the maximum value of the vibration velocity is 2.4 mm/s. It was confirmed that the vibration level of the proposed system is significantly low.**


## I. INTRODUCTION

Renewable energy systems, especially a wind turbine or a photovoltaic cell, generate power fluctuation depending on the meteorological conditions. Therefore, these systems require energy buffers, such as the electric double layer capacitors (EDLC), batteries, or flywheels to suppress the power fluctuations. One of the problems in the battery or the capacitor energy storage is short of life time. In particular, the lifetime depends on the ambient temperature and the numbers of charge and discharge time. In addition, the battery cannot carry up with rapid charge and discharge by a large internal resistance. On the other hand, the EDLC provides high charge and discharge efficiencies. Moreover, the rapid of charge and discharge is possible because the internal resistance is very small. However, similar to the battery, the lifetime is decreased due to the influence of the ambient temperature. In contrast, the flywheels are environmental friendly and low maintenance cost. Furthermore, the flywheel has a long lifetime due to no chemical structure, thus the charge and discharge characteristics have high cycle and high performance. Additionally, the kinetic energy which stored in the flywheel is proportional to the square of the rotational speed. For this reason, ultra high speed rotation using magnetic bearings have been studied in order to achieve high energy density [1-6]. The magnetic bearing to hold the rotating shaft without mechanical contact has been studied. However, the structure of the flywheel results in costly. Therefore, it is necessary to reduce the cost and simplify the structure of the flywheel system in order reaching towards the realization of a practical system.

This paper presents and discusses a low cost flywheel system with a regeneration power functions for the power leveling system. The flywheel system is configured from numbers of commercial products; which are consisting of a transducer, a general purpose inverters and an inexpensive microcomputer without the specific device. However, the inexpensive power detection device has a long time delay. As a result, the long delay time causes the control becomes unstable. In this study, in order to improve the response performance of the regenerative power, time delay compensation scheme based on the Smith predictor [7] is applied to the proposed flywheel system. In addition, the proposed system uses low cost ball bearings insteads of expensive magnetic bearings. Therefore, the vibration of the flywheel should be evaluated in terms of environmental friendly.

In this paper, the effectiveness of the proposed flywheel system is evaluated from the viewpoint of the following subjects.

(i)A Response performance of the power control

In the method of controlling the instantaneous power that is conventionally used, exclusive design of the inverter is essential because the high-speed response performance is

required. On the other hand, in the proposed system, the custom inverter is not required because a standard transducer from the market is applied into the power detection. However, the detection of time by inexpensive transducer may lead to instability of the power control system. Therefore, the control performance is improved by applying the Smith predictor into the power control system.

(ii) Effectiveness of the power leveling control

Power fluctuation of solar power is reproduced by using the step-down chopper. In addition, the effectiveness the proposed system as a power leveling system is confirmed in experiments.

(iii) Vibration characteristics

In this study, flywheel is applied to compensate the power fluctuations, such as solar power and wind power. Therefore, the flywheel system will install in the vicinity of the place of residence areas. Therefore, low vibration and low noise operation is required. However, since the flywheel is rotating machine, it generally produces a larger vibration comparing to the battery or EDLC. Therefore, the vibration characteristics during power leveling operation are evaluated by the experiment.

## II. Prototype Flywheel System

Fig. 1 shows the photograph of the proposed flywheel system of which has the specifications as shown in Table 1. The general purpose ball bearings is used to reduce the costs and to improve the performance at the rotational speed within 9500 r/min. Moreover, the outward form of the flywheel is 569×511×600 mm, and the energy density is 17.2 kJ/dm$^3$.

Fig. 2 shows the block diagram of the prototype flywheel system including the accessories parts. Inexpensive power meters which has a long time delay is applied in this system. Additionally, the rotational speed command of the flywheel is controlled by an inexpensive PIC microcontroller. In addition, the vacuum pump and the oil cooler are implemented to reduce the windage loss and heat generation. As a part of the mechanical features, a small vacuum pump is implemented because the flywheel has been stored in a sealed container. In this structure, it is possible to reduce the windage loss which occurs at high speed rotation region. Furthermore, over temperature of the bearing and the motor can be prevented by the oil cooler.

Note that this flywheel system assumes that several numbers of flywheels are used in one system in order to increase energy capacity. Therefore, an oil pump and a vacuum pump can be used for some flywheels.

In addtion, the loss analysis of the prototype flywheel system is evaluated.

Fig. 3 shows the analytical result of the steady state losses. In this experiment, the rotation speed is 9500 r/min, the vacuum is kept at 800 Pa. As a result, the flywheel losses in the steady state are as follows; the bearing loss is 19 %, the iron loss is 76 % for the induction motor. From the analysis, it is confirmed that the motor loss is dominant in the standby mode. Therefore, it is necessary to reduce the motor loss in order to improve the efficiency of the flywheel system.

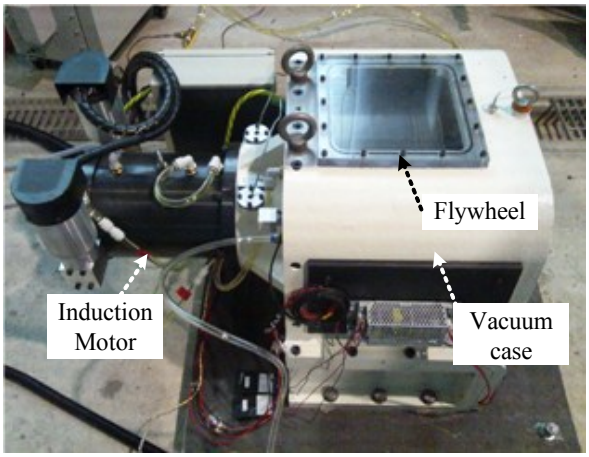


Fig. 1. Photograph of the prototype Flywheel System. This system uses low cost flywheel and the general purpose products.

Table 1. Specification of the Flywheel unit.

| | |
|---|---|
| Rated voltage | 200V |
| Rated current | 126A |
| Rated rotation speed | 9500rpm |
| Accumulated energy | 3.0MJ |
| Outward form | 569×511×600mm |
| Energy density | 17.2kJ/dm$^3$ |
| Weight of the FW | 241kg |
| Diameter of the FW | 45cm |

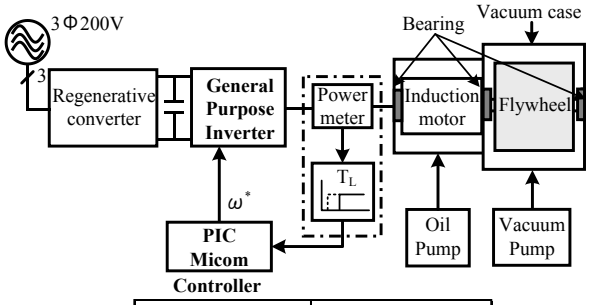


| | |
|---|---|
| **Inverter** | **FRENIC5000G11** |
| **Controller** | **PIC16F887** |
| **Sampling Time** | **20ms** |
| **Delay Time $T_L$** | **400ms** |

Fig. 2. Configuration of the Flywheel system including the accessories parts.

## III. POWER CONTROL METHOD WITH SMITH PREDICTOR

In the flywheel system, when induction machine is operated as a generator during deceleration, kinetic energy is converted into the electrical energy. On the other hand, during acceleration, the electrical energy is stored as kinetic energy, which is working as a motor. In general, inexpensive general purpose inverter can only provide speed command. Therefore, the charging and discharging power is controlled by the speed of the flywheel.

The kinetic energy of a body of revolution is expressed by (1).

$$E = \frac{1}{2} J\omega^2 \quad \text{.....(1)}$$

where, $J$ is the moment of inertia[kgm$^2$] and $\omega$ is the angular velocity of the body revolution[rad/s]. In addition, the speed command $\omega^*$ which shown in Fig. 2 can be obtained by transforming (1).

On the other hand, the output power of the flywheel can be obtained by differentiating the both sides of (1) from the relation between the rotational kinetic energy and power. Thus, the output power is expressed by (2).

$$P = J\omega \frac{d\omega}{dt} \quad \text{.....(2)}$$

Accordingly, the regenerative power of the flywheel is proportional to the product of the rotational angular velocity and angular acceleration. The speed command value for the regenerative power of the flywheel is given by (3).

$$\omega^* = \frac{1}{J} \int \frac{P^*}{\omega_o} dt \quad \text{.....(3)}$$

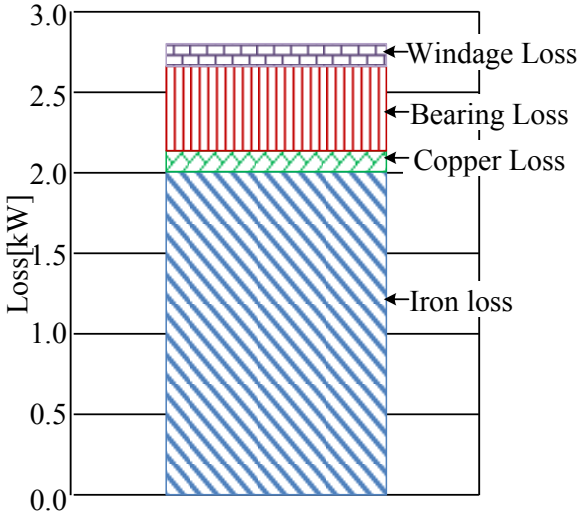


Fig. 3. Analytical results of the steady state losses. The rotation speed is 9500 r/min, the vacuum is kept at 800 Pa.

where, $\omega_o$ is the rotational angular velocity of the previous sampling time and $P^*$ is the output of the PI controller.

Furthermore, the discrete system of equation (3) is given by (4).

$$\omega_n = \omega_{n-1} + \frac{1}{J} \frac{P^*}{\omega_{n-1}} \Delta t \quad \text{..... (4)}$$

where,$\omega_{n-1}$ is the speed command value of the previous sampling time and $\Delta t$ is the sampling time of the controller.

In this system, the regenerative power is obtained from an inexpensive power meter that has a sampling time of 400 msec. In such a system, the control may become unstable by setting a high proportional gain to improve the response. In this paper, the control performance is improved by the Smith delay time compensation scheme.

Fig. 4(a) shows the block diagram of the typical feedback control system. Note that the change of the rotational angular velocity is sufficiently slower than the processing time of the control system. Therefore, the rotational angular velocity of the previous sampling time is treated as a constant value $\omega_o$. The characteristic equation of this control system is given by (5).

$$1 + C(s)G(s)e^{-T_L S} = 0 \quad \text{..... (5)}$$

In a typical feedback control system, the system becomes unstable due to the phase lag. This is caused by the time delay.

Fig. 4(b) shows the block diagram with the Smith predictor. This compensation eliminates the effect of delay time by estimating the output of the controlled object $G(s)$ after the

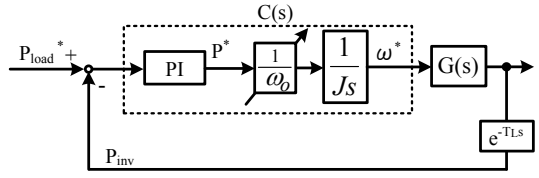


(a)Without smith predictor.

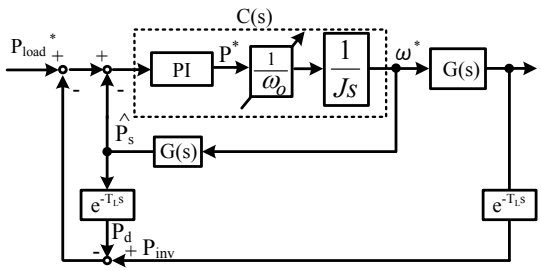


(b)With smith predictor.

Fig.4. Block diagram of time delay compensation scheme based on Smith predictor. This compensation eliminates the effect of time delay by estimating the output of the controlled object $G(s)$ after the lapse of time delay.

lapse of delay time. The characteristic equation is given by (6).

$$1 + C(s)G(s) = 0 \quad \text{.....(6)}$$

Therefore, the control performance can be improved from this equation. In other words, the delay time element has been removed from the characteristic equation.

In this control system, the speed command $\omega^*_{\wedge}$ is obtained by (2) from the estimation of the output power $P_s$. Note that $P_{inv}$ is detected value of the power meter and $P_d$ is the output power after the lapse of dead time. In addition, $P_s$ is calculated by the inertia $J$ and the rotation speed command $\omega^*$ from (1).

## IV. Simulation and Experimantal Verifications

Fig. 5 illustrates the simulation results of the regenerative power from the flywheel system with and without the Smith predictor. The simulation conditions are as follows; the steady rotation speed is 6000 r/min and the load is changed from 0.0 kW to 2.0 kW. From the simulation results of Fig. 5(a), a large overshoot occurs when the Smith predictor is not applied. By contrast, Fig. 5(b) shows that the overshoot does not occur when the Smith predictor is applied. Therefore, it is confirmed that the response performance is improved by the Smith predictor.

Next, the effectiveness of the Smith predictor is verified by the experiment.

Fig. 6 shows the step response of the output power. Note that the experimental conditions are similar to the simulation.

In addition, the gain of PI controller is determined by the limit sensitivity method [8]. The inverter used in the experiment is FRENIC5000G11 (*Fuji Electric*), the microcontroller is PIC16F887 (*Microchip Technology*), and the sampling time is 20msec.

According to Fig. 6(a), an overshoots is approximately 500 W because the power measurement system has a time delay. On the other hand, it is confirmed that the overshoots does not occur by using Smith predictor in Fig. 6(b). From these results, the effectiveness of the compensator is confirmed in simulations and experiments.

Fig. 7 shows the frequency characteristics of the prototype system. From the results, frequency response after applying the Smith predictor is 0.18Hz. Power generation system using renewable energy power generator varies greatly depending

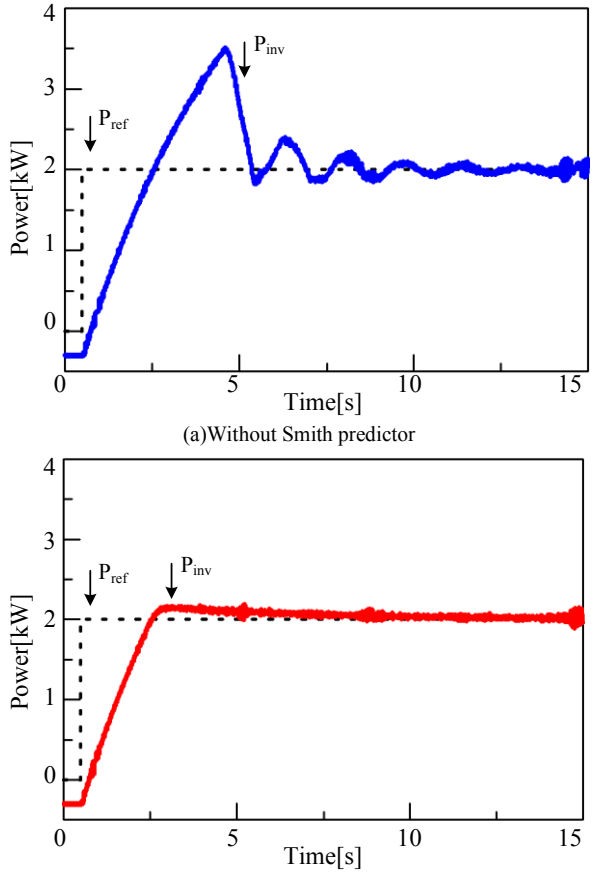


Fig. 5. Step response of the regeneration power on the simulation results. The steady rotation speed is 6000 r/min and the load is changed from 0.0 kW to 2.0 kW.

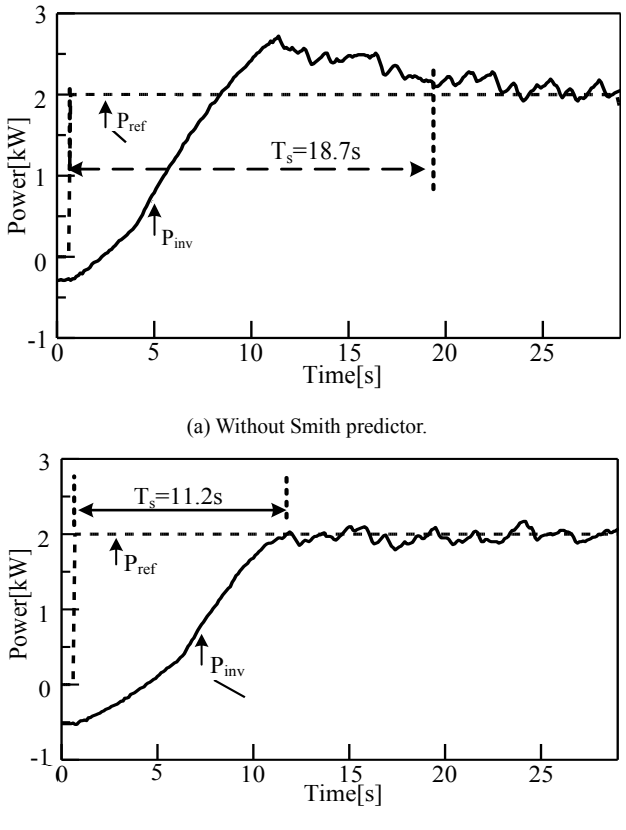


Fig. 6. Step response of the regeneration power on the experimental results. The rotation speed is 6000 r/min and the load is changed from 0.0 kW to 2.0 kW.

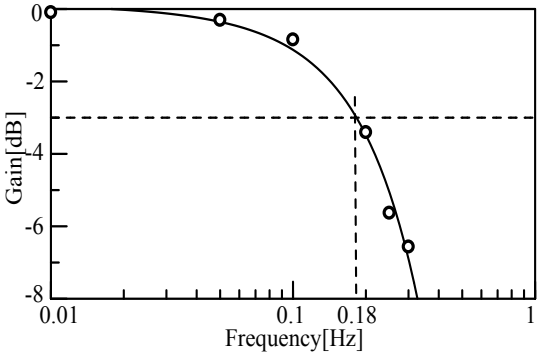


(a)Gain characteristic.

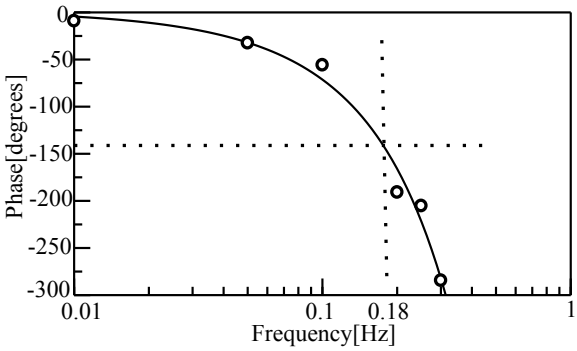


(b)Phase characteristic.

Fig. 7. Bode diagrams of the proposed control system.

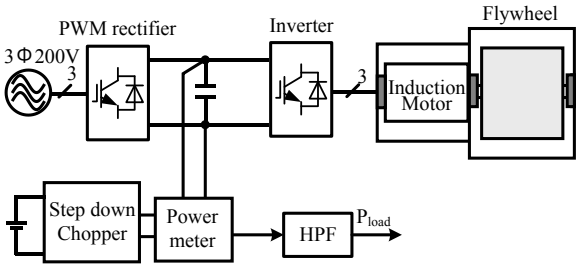


Fig. 8. Configuration of the experimental system for the power fluctuation compensation.

on the weather conditions. Therefore, the prototype system can be applied to compensate for power fluctuations which is several tens of seconds [9][10].

## V. Verification of Power Leveling Control

Fig. 8 shows the power leveling control system. Note that the rotation speed is 5500 r/min at steady state. In the experiment, the power fluctuation is reproduced by a step-down chopper. In addition, the flywheel power command value is extracted from a high pass filter (HPF) that the cutoff frequency is set to 0.0025 Hz. The prototype system is intended to compensate for a short cycle of the power fluctuation. Therefore, the cutoff frequency of the HPF is set to low frequency.

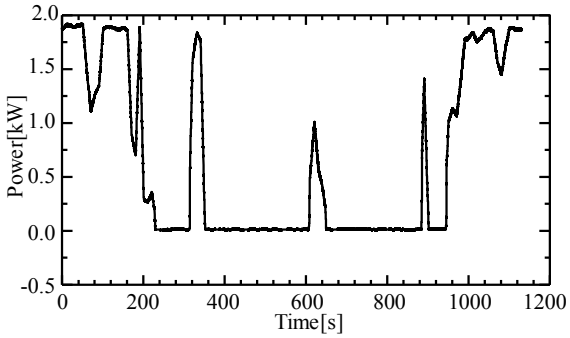


(a)Fluctuation pattern

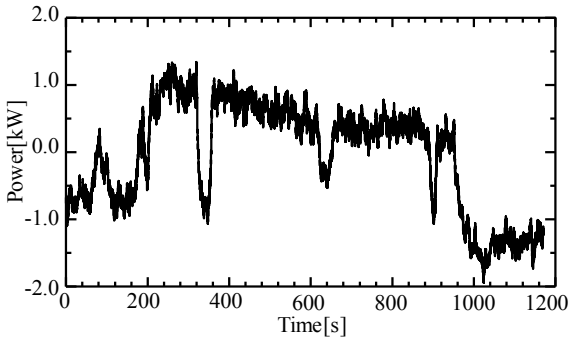


(b)Output power of the Flywheel

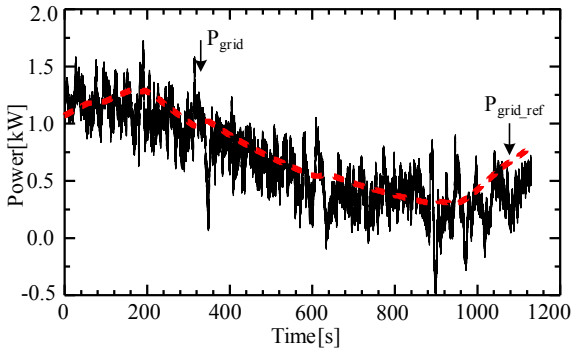


(c) Grid power

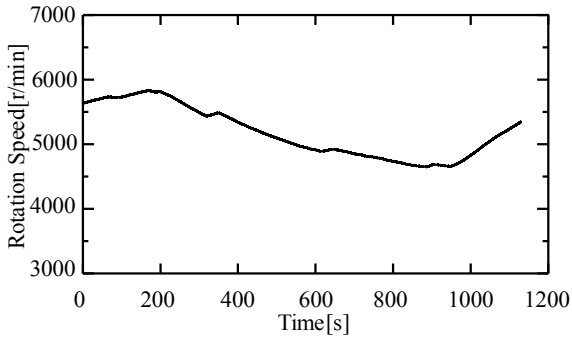


(d)Rotation speed

Fig. 9. Experimental results of the power fluctuation compensation control when applying Smith predictor.
(Rotation speed is 5500r/min)

Fig. 9(a) shows the power fluctuation pattern which uses as a part of generation power by PV panels. From this figure, the generation power of the solar cell has a rapid power fluctuation of approximately 2 kW.

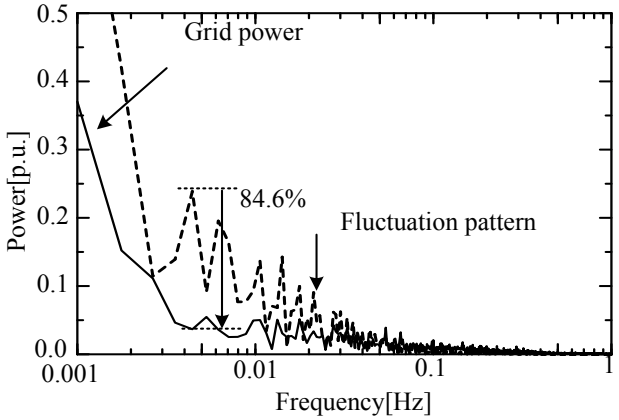


Fig.10. Harmonic analysis during the power fluctuation compensation. The experimental conditions are similar to Fig. 9.

Fig. 9(b) shows the output power of the flywheel and Fig. 9(c) shows the grid power. From these results, the fluctuation of generated power is compensated by the output power of the flywheel. Therefore, the power fluctuation is noticed not occurring in the grid power.

Fig. 9(d) shows the rotation speed of the flywheel. As a result, it is confirmed that the sudden speed variation does not occurs. According to the Fig. 9(c), the high frequency ripple occurs in the grid power. This ripple is caused by the influence of the time delay error. This problem can be improved by the optimization of the control gain.

Fig. 10 shows the harmonic analysis of the fluctuation pattern and the grid power. The experimental conditions are similar to Fig. 9. As the result, it is confirmed that the fluctuation pattern has large frequency component between 0.01 Hz and 0.004 Hz. By contrast, the grid power fluctuations over 0.004 Hz is reduced by 84.6 % in the power leveling control.

## VI. VIBRATION ANALYSIS

In this study, the flywheel is applied as a power compensator for the solar power and wind power. The flywheel system will be installed in the residence areas as therefore low vibration and low noise operations are preferable. The vibration characteristics during power leveling operation are evaluated by the experiment.

Fig. 11 shows the mounting position of the acceleration sensor used for vibration analysis. In the experiment, acceleration in the radial direction and axial direction are measured with respect to the axis of rotation of the flywheel. In addition, DS-3000(*Ono Sokki*) is used as the acceleration sensor in the analysis and data acquisition.

Fig. 12(a) shows the vibration velocity in the radial direction, Fig. 12(b) shows the vibration velocity in the axial direction. where, the experimental conditions are the same as the operation of the power fluctuation compensation. In addition, the vibration velocity is calculated by integrating the acceleration measured from the acceleration sensor. From these results, the vibration velocity in the axial direction is larger than the radial direction of the flywheel. The maximum value of the vibration velocity is 2.4 mm/s. According to the standard of JIS, the prototype system is classified as zone B which vibration velocity is between 1.12 mm/s to 2.8 mm/s. In this zone, long-term operation is possible without any restriction. In addition, the vibration velocity is increased rapidly at a rotational speed of 5200 r/min in the axial direction. The vibration becomes large at the number of revolutions of the same when changing the power fluctuation pattern. Therefore, it is a resonance phenomenon due to the natural frequency of the system.

Next, the causes of vibration are considered and the following four points show the reasons of vibration in the flywheel [11].

(i) The vibration caused by the imbalance of mass distribution of the rotor axis,

(ii) The vibrations due to the deviation of the center line of the rotary shaft which is connected by a shaft coupling,

(iii) The vibration caused by the electromagnetic force of the induction machine,

and (iv) The vibration caused by the rolling elements of the bearing.

From the past studies, the element of (i), (ii), (iii) appears prominently in the vibration velocity. The vibration caused by the imbalance of mass distribution of the rotor appears as the rotational frequency component in the radial direction. In addition, the vibrations due to the deviation of the center line of the rotary shaft which is connected by a shaft coupling appear to be larger as the order component and the rotation frequency in the axial direction are increasing. Moreover, the vibration caused by the electromagnetic force of the motor is generated by the magnetic attraction force of the rotor and the stator. This vibration appears as a frequency component of twice the power supply frequency. Therefore, the causes of vibration that occurs in the prototype system are analyzed by harmonic analysis.

Fig. 13 shows the harmonic analysis results at maximum vibration velocity in each of the direction. From Fig. 13(a), the radial direction is dominated by the vibration of the rotational frequency component. This is the vibration caused by unbalanced mass of rotating axis. In addition, the vibration of 13 kHz is a vibration due to torque ripple because it is equal to the carrier frequency. Moreover, the vibration of 550 Hz is the natural frequency component of the system. From Fig. 13(b), the axial direction is dominated by the rotational frequency component. This is the vibration caused by the displacement of the center shaft coupling. From these results, the component of twice the power supply frequency is 0.2 mm/s or lesser in both the directions. Therefore, the influence

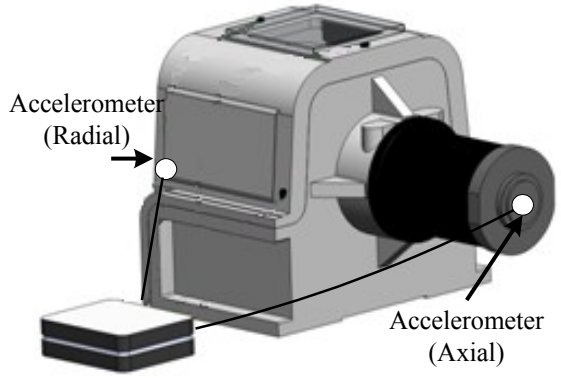


Fig.11. Mounting position of the accelerometer.

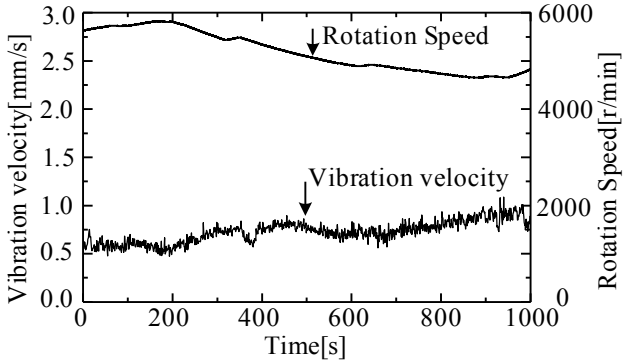


(a) Radial direction

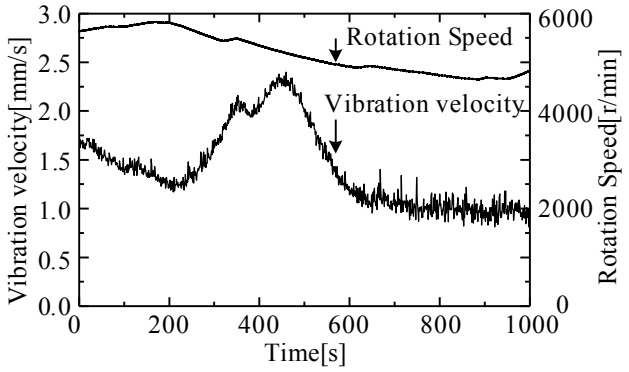


(b) Axial direction

Fig.12. Analysis of the vibration velocity during the power fluctuation compensation control.

of the vibration caused by the electromagnetic force of the motor is very small.

Fig. 14 shows the harmonic analysis result at maximum vibration acceleration. In general, the bearing vibration appears as the acceleration of the high frequency component. Therefore, the factor of high frequency vibration is evaluated by the acceleration analysis. The frequency component of the vibration that is caused by the bearing can be calculated from the rotational frequency and dimensions of the bearing [12]. The frequency component of the vibration generated by the rolling elements of the bearing is expressed by (7).

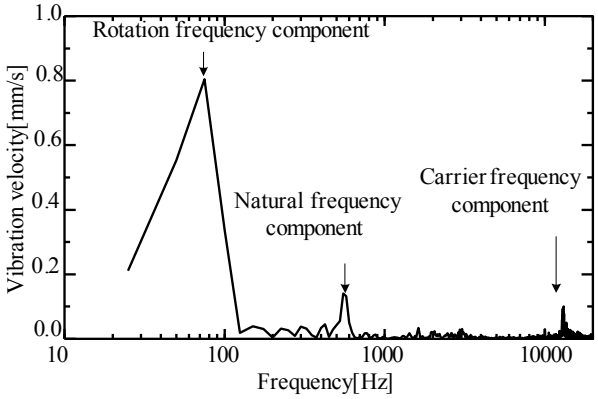


(a)Radial direction

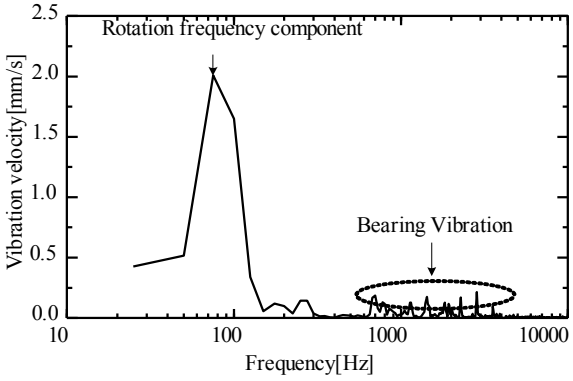


(b) Axial direction

Fig.13. Harmonic analysis results at maximum vibration velocity in each direction.

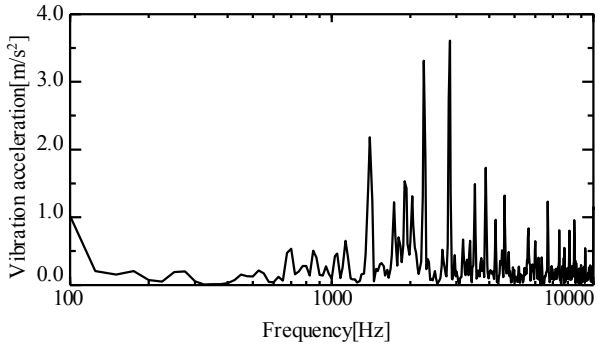


Fig.14. Harmonic analysis result at maximum vibration acceleration. (Axial direction)

$$f_c = \frac{f_r}{2}\left(1 - \frac{d}{D}\cos a\right) \quad \text{.....(7)}$$

where, $f_r$ is rotational speed of the shaft, $d$ is the diameter of the rolling element, $D$ is the pitch circle diameter of the bearing and α is the contact angle.

In this system, the vibration of the bearing appears as a component 10.57 times, 12.43 times and 14.92 times of the rotation frequency. From the harmonic analysis, the vibration appears as a component 11.88 times, 12.90 times, 15.50 times

as large as the rotation frequency. Therefore, the analysis results are almost identical with the theoretical value. The amplitude of the high order component is greater due to the resonance with the natural frequency of the system. From these analysis, it is confirmed that the main factor of the high frequency component is the vibration of the ball bearings.

## VII. CONCLUSION

This paper discussed a low cost power leveling system with a 3 MJ, 9500 r/min flywheel energy storage. In this system, the control performance is improved by applying the Smith compensator. From the step response of power, it is confirmed that the overshoot of the power does not occur and the settling time is reduced.

The loss analysis of the system is demonstarated. From the analysis, it is confirmed that the motor loss is dominant in the standby mode. Therefore, it is necessary to apply the permanent magnet synchronous motor with low loss for further efficiency of the flywheel system.

Furthermore, the effectiveness of the control for the prototype system is evaluated in term of vibration analysis. From the analysis, it is confirmed the main factors that cause the vibration are (i) the unbalance of the flywheel and (ii) the rolling element of the ball bearings. Therefore, it is possible to further suppress the vibration by adopting a pivot bearings to reduce the mechanical contact and improve the machining accuracy.

## ACKNOWLEDGMENT

A part of this study was supported by Industrial Technology Grant Program in 2011 from New Energy and Industrial Technology Development Organization (NEDO) of Japan.

## REFERENCES

[1] M. Strasik, P. E. Johnson, A. C. Day, J. Mittleider, M. D. Higgins, J. Edwards, J. R. Schindler, K. E. McCrary, C. R. McIver, D. Carlson, J. F. Gonder, and J. R. Hull:" Design, Fabrication, and Test of a 5-kWh/100-kW Flywheel Energy Storage Utilizing a High-Temperature Superconducting Bearing", IEEE Transactions on Applied Superconductivity., Vol. 17, No.2, pp.2133-2137(2007)

[2] Frank N. Werfel, Uta Floegel-Delor, Thomas Riedel, Rolf Rothfeld, Dieter Wippich, Bernd Goebel, Gerhard Reiner, and Niels Wehlau:"A Compact HTS 5 kWh/250 kW Flywheel Energy Storage System",IEEE Transactions on Applied Superconductivity,Vol.17,No.2, pp.2138-2141(2007)

[3] Barbara H. Kenny, Peter E. Kascak, Ralph Jansen, Timothy Dever, and Walter Santiago:"Control of a High-Speed Flywheel System for Energy Storage in Space Applications", IEEE Transactions on Industry Applications, Vol.41, No.4, pp.1029-1038 (2005)

[4] Z. Kohari, Z. Nadudvari, L. Szlama, M. Keresztesi, and I. Csaki:"Test Results of a Compact Disk-Type Motor/GeneratorUnit with Superconducting Bearings for Flywheel Energy Storage Systems with Ultra-Low Idling Losses", IEEE Transactions on Applied Superconductivity,, Vol.21, No.3, pp.1497-1501(2011)

[5] Frank N. Werfel, Uta Floegel-Delor, Thomas Riedel, Rolf Rothfeld, Dieter Wippich, Bernd Goebel, Gerhard Reiner, and Niels Wehlau:"Towards High-Capacity HTS Flywheel Systems", IEEE Transactions on Applied Superconductivity, Vol.20, No.4, pp.2272-2275 (2010)

[6] C. Zhang, K.J. Tseng, T.D. Nguyen, S. Zhang : "Design and loss analysis of a high speed flywheel energy storage system based on axial-flux flywheel-rotor electric machines", IPEC-Sapporo, pp.886-891(2010)

[7] J. Shibata, K. Ohishi, I. Ando, M, Ogawa: "Fine output voltage control for inverter system having nonlinear load and time-delay", IPEC-Sapporo, pp.1541-1546(2010)

[8] J.G Zieglae and N.B. Nicholes, "Optimum settings for automatic controllers", Trans, ASME, 64, pp.759–768(1942)

[9] S. M. Muyeen, Rion Takahashi, Toshiaki Murata, and Junji Tamur:" Integration of an Energy Capacitor System with a Variable-Speed Wind Generator", IEEE Transactions on Energy Conversion,, Vol.24, No.3, pp.740-749(2009)

[10] Bingchang Ni, Constantinos Sourkounis:" Energy Yield and Power Fluctuation of Different Control Methods for Wind Energy Converters", IEEE Transactions on Industry Applications, Vol.47, No.3, pp.973-978(2011)

[11] K. Izawa, S. Ichikawa," Development Report for High Speed Flywheel", JAXA Research and Development Report(2008)

[12] H. Talii, "Trends of Rolling Bearing Performance and Recent Results", Koyo Engineering Journal, No.163 (2003)